

## YBa<sub>2</sub>Cu<sub>3</sub>O<sub>7</sub> microwave resonators for strong collective coupling with spin ensembles

A. Ghirri,<sup>1(a)</sup> C. Bonizzoni,<sup>2</sup> D. Gerace,<sup>3</sup> S. Sanna,<sup>3</sup> A. Cassinese,<sup>4</sup> and M. Affronte<sup>2</sup>

<sup>1</sup>Istituto Nanoscienze - CNR, Centro S3, via Campi 213/a, 41125 Modena, Italy

<sup>2</sup>Dipartimento Fisica, Informatica e Matematica, Università di Modena e Reggio Emilia and Istituto Nanoscienze - CNR, Centro S3, via Campi 213/a, 41125 Modena, Italy

<sup>3</sup>Dipartimento di Fisica, Università di Pavia, via Bassi 6, 27100 Pavia, Italy

<sup>4</sup>CNR-SPIN and Dipartimento di Fisica, Università di Napoli Federico II, 80138 Napoli, Italy

(Received 23 February 2015; accepted 29 April 2015; published online 7 May 2015)

Coplanar microwave resonators made of 330 nm-thick superconducting YBa<sub>2</sub>Cu<sub>3</sub>O<sub>7</sub> have been realized and characterized in a wide temperature ( $T$ , 2–100 K) and magnetic field ( $B$ , 0–7 T) range. The quality factor ( $Q_L$ ) exceeds  $10^4$  below 55 K and it slightly decreases for increasing fields, remaining 90% of  $Q_L(B = 0)$  for  $B = 7$  T and  $T = 2$  K. These features allow the coherent coupling of resonant photons with a spin ensemble at finite temperature and magnetic field. To demonstrate this, collective strong coupling was achieved by using di(phenyl)-(2,4,6-trinitrophenyl)iminoazanium organic radical placed at the magnetic antinode of the fundamental mode: the in-plane magnetic field is used to tune the spin frequency gap splitting across the single-mode cavity resonance at 7.75 GHz, where clear anticrossings are observed with a splitting as large as  $\sim 82$  MHz at  $T = 2$  K. The spin-cavity collective coupling rate is shown to scale as the square root of the number of active spins in the ensemble. © 2015 AIP Publishing LLC. [<http://dx.doi.org/10.1063/1.4920930>]

Thanks to pioneering experiments and theoretical proposals, quantum technologies have enormously advanced and the interest can now be turned to explore viable routes for practical applications. Several pure quantum systems, including cold atoms, photons, superconducting qubits, spin impurities in Si, or nitrogen vacancies (NV) in diamond—among many others—have been deeply investigated in the last decade as potential candidate qubits for applications in quantum information processing, and techniques for their read out and manipulation have been developed.<sup>1</sup> Advantages and limitations of each system have been debated: whilst large margins of improvement are still possible for the different techniques, fundamental limits are clear for each system. A possible strategy to overcome these barriers is to combine quantum systems of different nature and take advantage of the best features of each of them in hybrid quantum devices. Of course, this opens new technological challenges. Along these lines, high-quality factor resonators play a pivotal role, since photons can be coupled with a number of other two-level systems (qubits) while begin optimal flying quantum bits themselves. Among them, planar resonators are particularly suitable to be coupled with a variety of atomic or solid state qubits, with the final goal of developing an on-chip hybrid quantum technology.<sup>1,2</sup> In fact, mm-length microwave resonators can be routinely fabricated in a scalable arrangement and on different substrates. In particular, state-of-art superconducting resonators allow the achievement power-independent quality factors as high as  $10^6$  or above in planar geometry at the single photon level.<sup>3,4</sup>

A key step to coherently transfer information between cavity photons and stationary qubits is to achieve the strong coupling regime: electric or magnetic dipole coupling between the qubit and the confined electromagnetic field

should overcome their respective damping rates.<sup>5</sup> Electric dipole coupling allowed the observation of the strong coupling with single quantum emitters.<sup>6–9</sup> On the other hand, spin ensembles collectively coupled to microwave resonators have been proposed for a hybrid quantum technology.<sup>11</sup> Since the magnetic dipole coupling of a single spin to a resonator mode,  $g_s$ , is typically too small, a collective enhancement of the effective coupling rate of  $N$  spins,<sup>10</sup> scaling as  $g_s\sqrt{N}$ , allows to overcome the limitations due to both the decoherence rate of the spin system,  $\gamma_s$ , and the inverse photon lifetime in the cavity,  $\kappa = \omega_0/Q$  (where  $f_0 = \omega_0/2\pi$  is the resonant frequency and  $Q$  is the resonator quality factor).<sup>12</sup> In this way, collective strong coupling of spin ensembles and microwave photons has been experimentally shown in coplanar resonators,<sup>13–15</sup> three-dimensional (3D) cavities,<sup>19–22</sup> and microwave oscillators.<sup>23</sup> While 3D resonators are less suited for on-chip integration, all of the previous achievements employing planar resonators were obtained with conventional superconductors (typically Nb), which are limited to operate at moderate magnetic fields. However, manipulation of spins may need application of finite magnetic fields.<sup>29,30</sup> Microwave resonators made of high  $T_c$  superconductors, such as YBa<sub>2</sub>Cu<sub>3</sub>O<sub>7</sub> (YBCO), have shown excellent performances from liquid nitrogen temperatures<sup>24–27</sup> down to mK range and single-photon regime.<sup>28</sup> Thanks to the large value of their intrinsic upper critical field, these systems offer unprecedented possibilities for spin manipulation.

In this letter, we show that YBCO coplanar resonators have excellent performances under strong magnetic fields, with quality factors significantly exceeding  $10^4$  up to  $T \sim 55$  K. Therefore, they appear as a significant step ahead for quantum technology applications. Stimulated by recent theoretical<sup>19,31</sup> and experimental<sup>19,20,23</sup> results, here we focused on the high photon number and high temperature regimes, where we report

<sup>a)</sup>Electronic mail: alberto.ghirri@nano.cnr.it.

the strong collective coupling of an electron spin ensemble to YBCO microwave coplanar resonators. Our major interest is to use molecular spins, which offer several advantages with respect to spin impurities.<sup>32</sup> Interesting and sufficiently long phase memory times have been reported for simple radicals,<sup>33,34</sup> mono-metallic Cu phthalocyanine molecules,<sup>35</sup> or (PPh<sub>4</sub>)<sub>2</sub>[Cu(mnt)<sub>2</sub>] derivatives.<sup>36</sup> In the present work, we employed commercial di(phenyl)-(2,4,6-trinitrophenyl)iminozanium (DPPH), which is regularly used as field calibration marker in EPR spectroscopy. The decoherence time of DPPH is  $T_1 = T_2 = 62$  ns,<sup>16</sup> while the continuous wave linewidth is sharp ( $\gamma_s/2\pi \simeq 3.9$  MHz)<sup>17</sup> due to the exchange narrowing effect. Below 10 K, the linewidth increases as an effect of anti-ferromagnetic interactions [ $\gamma_s/2\pi \simeq 14$  MHz at 2 K].<sup>18</sup> The strong coupling between DPPH radicals and a confined microwave field has been already demonstrated with 3D cavities<sup>19,20</sup> or microwave oscillators.<sup>23</sup>

Superconducting resonators were fabricated by optical lithography upon wet etching (2% H<sub>3</sub>PO<sub>4</sub> solution) of commercial 10 × 10 mm<sup>2</sup> double sided YBCO films (330 nm thick) on sapphire (430 μm) substrates (Ceraco GmbH). The film is gold-coated on the back side to improve the contact to ground. The patterned coplanar structure is constituted by a 8 mm central strip having width  $w = 200$  μm and separation  $s = 73$  μm from the lateral ground planes [Fig. 1(d)].<sup>24</sup> The coupling of the resonator to the feed line can be adjusted by finely tuning the position of the launchers. We tested five YBCO planar resonators finding quite reproducible results.<sup>37</sup> Low temperature measurements were performed using a Quantum Design PPMS cryo-magnetic system equipped with 7 T magnetic field applied parallel to the plane of the resonator. Reflection [ $S_{11}(f)$ ] and transmission [ $S_{21}(f)$ ] scattering parameters were measured by means of an Agilent PNA Vector Network Analyzer (VNA).

We first show that coplanar resonators made of YBCO allow expanding temperature, magnetic field, and power ranges with respect to the Nb cavities commonly used in circuit-QED experiments. At  $T = 2$  K, the transmission spectrum shows a well defined resonance centered at  $f_0 = 7.7553$  GHz [Fig. 1(a)]. The resonance dip is visible also in the  $S_{11}(f)$  spectrum. This indicates that the resonator is not undercoupled, and that the loaded quality factor ( $Q_L$ ) should be considered. Since  $S_{21}(f) = 20 \log_{10}(\sqrt{P(f)/P_{inc}})$ , where  $P(f)$

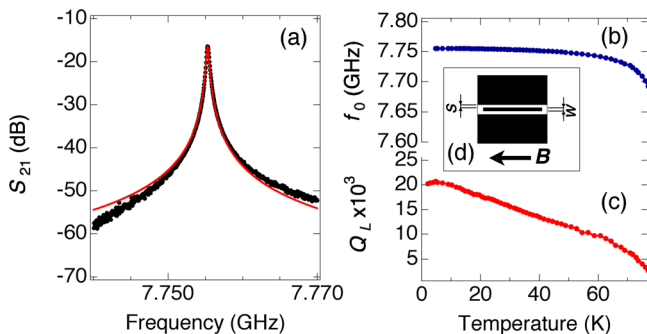


FIG. 1. Characteristics of bare YBCO resonators. (a) Transmission spectrum measured at  $T = 2$  K and  $B = 0$ . The input power is  $P_{inc} = -22.5$  dBm. The red line shows the calculated curve. Temperature dependence of the (b) resonance frequency,  $f_0$ , and (c) loaded quality factor,  $Q_L$ . In the inset (d), a sketch of the YBCO coplanar resonator is shown.

and  $P_{inc}$  are the transmitted and the input powers at the capacitor of the resonator, respectively,<sup>37</sup> the transmission spectrum can be fitted by<sup>25</sup>

$$S_{21}(f) = -IL - 10 \log_{10} \left[ 1 + Q_L^2 \left( \frac{f}{f_0} - \frac{f_0}{f} \right)^2 \right], \quad (1)$$

where  $Q_L(2\text{ K}) \simeq 20000$  and the insertion loss is  $IL = -S_{21}(f_0) = 16.5$  dB [red line in Fig. 1(b)]. The quality factor corresponds to that calculated from the half power bandwidth (3-dB method). More decoupled resonators display stable  $Q_L > 30000$  in the high power regime.<sup>37</sup>

The temperature dependence of the transmission resonance was investigated by measuring  $S_{21}(f)$  in the range of 2–100 K. To extract  $f_0$  and  $Q_L$ , we fitted each spectrum with Eq. (1). Figure 1(b) shows a small shift of  $f_0$  between 2 and 60 K. For higher temperature, the resonance peak shifts towards lower frequencies, and it disappears in correspondence to the YBCO film critical temperature ( $T_c = 87$  K). The loaded quality factor [Fig. 1(c)] progressively decreases with increasing  $T$ , while remaining  $Q_L(T) > 10000$  for  $T < 55$  K. This behavior is in line with similar results reported in the literature.<sup>24</sup>

An applied magnetic field ( $B$ ) generally gives rise both to a decrease of the quality factor and to a hysteretic behavior of the resonant frequency. While this behavior was effectively observed for intermediate temperatures,<sup>37</sup> at low temperature, the field dependence becomes progressively weaker. Figure 2(a) shows a series of  $S_{21}(f)$  spectra measured at 2 K for increasing  $B$ , up to 7 T. The values of  $f_0$  and  $Q_L$  extracted from Eq. (1) are plotted as a function of  $B$  in (b) and (c): they are remarkably stable up to 7 T, being  $Q_L(7\text{ T}) = 0.90 \times Q_L(0\text{ T})$ . We notice that for Nb resonators, a drop of  $Q_L$  is observed for fields in the mT range.<sup>38</sup> Degradation of the quality factor of the superconducting resonators against the applied field is due to the dissipation mechanisms related to the vortex motion. This effect has been generally described in terms of increase of the surface resistivity ( $R_s$ ) under applied magnetic field, whilst recent experimental results have evidenced that more sophisticated models are required for thin films.<sup>39</sup> Surface resistivity measurements performed at 20 K by means of the dielectric resonator method have shown a weak dependence of  $R_s$  with respect to a dc field up to 5 T applied parallel to the YBCO

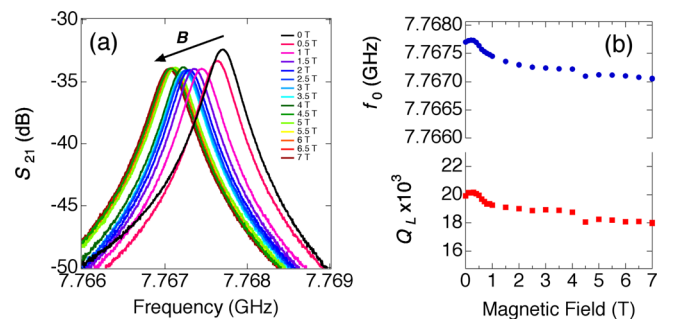


FIG. 2. (a) Transmission spectra as a function of frequency measured at 2 K for applied external magnetic fields up to 7 T. Dependence of (b) the cavity mode resonant frequency,  $f_0$ , and (c) the loaded quality factor,  $Q_L$ , on the externally applied magnetic field,  $B$ .

film.<sup>40</sup> These findings, independently obtained by different experimental techniques, corroborate the field dependence of  $Q_L$  we report in Fig. 2.

Summarizing the results of the YBCO resonators characterization, the decay rate of the cavity remains reasonably smaller than  $\kappa/2\pi \sim 1$  MHz in a wide temperature and magnetic field ranges, and we can therefore exploit these unique properties to perform circuit-QED experiments with spin ensembles as follows.

A thin layer of DPPH powder was attached to the center of the YBCO resonator by means of silicone grease. The volume of the sample ( $1.2 \times 0.5 \times 0.05$  mm<sup>3</sup>) was estimated under optical microscope, and it corresponds to a total number of approximately  $N \simeq 6 \times 10^{16}$  radicals.<sup>37</sup> In Fig. 3, we report the evolution of the transmission peak in correspondence to the resonance field of the DPPH spin ensemble ( $B_r \simeq 0.276$  T). At 2 K, two branches are observed, which indicate the presence of a large anticrossing between the resonator mode and the spin ensemble [Fig. 3(a)]. Cross-sectional  $S_{21}(f)$  spectra measured on resonance show two peaks separated by  $f_+ - f_- \simeq 82$  MHz [Fig. 3(b)]. The fit of the off-resonance (0.2694 T) spectrum with Eq. (1) gives  $f_0 = 7.7522$  GHz,  $Q_L = 16000$ , and  $IL = -33.5$  dB. Thus, the cavity decay rate results  $\kappa \simeq 0.5$  MHz, while the estimated number of photons inside the cavity mode volume<sup>41</sup> is  $N_{ph} \simeq 10^{11}$ . For increasing temperature, the width of the anticrossing decreases and the splitting is progressively reduced to  $\simeq 58$  MHz (at 5 K) and  $\simeq 39$  MHz (at 10 K) [Figs. 3(d) and 3(f)]. The splitting of the transmission peak in correspondence to the resonance field of DPPH is observed up to 50 K.<sup>37</sup> To evaluate the magnitude of the collective coupling constant  $g_c$ , we fitted the resonance frequency by using the usual expression for the vacuum field Rabi splitting

(neglecting the damping rates, i.e., the imaginary parts of the split eigenfrequencies)<sup>20</sup>

$$\omega_{\pm} = \omega_0 + \frac{\Delta}{2} \pm \frac{\sqrt{\Delta^2 + 4g_c^2}}{2}, \quad (2)$$

where  $\omega_{\pm} = 2\pi f_{\pm}$ ,  $\Delta = g\mu_B(B - B_r)/\hbar$ , and  $g = 2.0037$  is the Landé  $g$ -factor of DPPH. The fitted rates  $g_c/2\pi$  are plotted as a function of temperature in Fig. 4 (black circles), spanning from 39 MHz at 2 K to 9 MHz at 40 K. Hence, the strong coupling condition,<sup>1</sup>  $g_c \gg \gamma_s, \kappa$ , is clearly satisfied in our sample in the whole temperature range up to 40 K.

To interpret the results in Fig. 4, we notice that the number of polarized  $s = 1/2$  spins ( $N_p$ ) varies with temperature as

$$\frac{N_p}{N} = \tanh\left(\frac{hf}{2k_B T}\right). \quad (3)$$

Simultaneously,  $g_c$  rescales non-linearly as

$$g_c = g_s \sqrt{N_p}, \quad (4)$$

where  $g_s$  is the coupling of a single spin  $1/2$  to the resonator mode. In Fig. 4, we calculated the behavior of  $g_c$  by means of Eqs. (3) and (4) (solid red line). The best fit was obtained by means  $g_c/2\pi[\text{MHz}] = 134\sqrt{N_p/N}$ . From the zero temperature limit ( $N_p = N \sim 6 \times 10^{16}$ ) and the finite temperature values, we estimated a single-spin coupling rate in a restricted range  $g_s/2\pi \sim 0.55 - 0.60$  Hz. These values well compare with the one independently estimated from the known parameters of our resonators,<sup>37</sup> besides being consistent with the values reported in the literature for different cavity geometries and spin systems.<sup>1</sup> We also notice that even at the highest temperatures at which strong coupling can be observed, when only a small fraction of spins is coupled to the microwave mode, the condition  $N_{ph} \ll N_p$  still holds, for which Eq. (4) is a safe assumption.<sup>19</sup>

To get further insight about the  $g_c(N_p)$  dependence, we removed a portion of DPPH sample from the resonator and we repeated the measurements to extract the reduced coupling constant  $g_c^*(T)$ .<sup>37</sup> The remaining sample corresponds to approximately 75% of the original volume. The total number of  $s = 1/2$  radicals is thus reduced to  $N^* = 0.75 \times N$  and  $g_c^* = g_s \sqrt{0.75 \times N_p}$ . To compare these results with  $g_c(T)$ , in

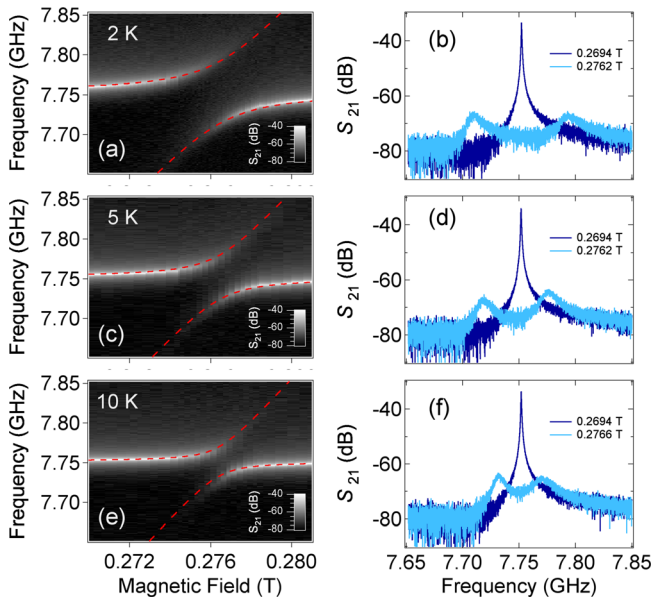


FIG. 3. Transmission spectra of a YBCO microwave resonator loaded with a DPPH spin ensemble ( $P_{inc} = -12.5$  dBm). The left column shows a series of two-dimensional maps obtained by plotting  $S_{21}(f)$  for different applied  $B$ . Temperatures: 2 K (a), 5 K (c), and 10 K (e). Dashed red lines display the calculated curves. The right column shows the cross sections related to the corresponding right panel, either on resonance (cyan) or off resonance (blue).

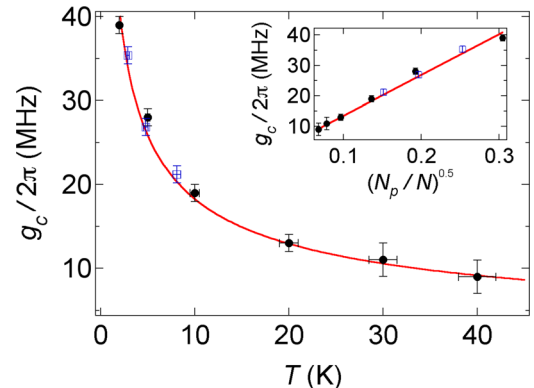


FIG. 4. Dependence of the collective coupling constant  $g_c(T)$  (black circles) with respect to  $T$  and  $\sqrt{N_p(T)/N}$  (inset). The blue open squares display  $g_c^*(T)/\sqrt{0.75}$ . Solid red lines show the calculated curves.

Fig. 4, we plotted the rescaled coupling constant  $g_c^*/\sqrt{0.75}$  as function of  $T$  and  $\sqrt{N_p/N}$  (open squares). The very good agreement between  $g_c^*(T)$  and  $g_c(T)$  corroborates the behavior described from Eqs. (3) and (4).

In summary, we have shown that YBCO microwave planar resonators constitute a viable route for the implementation of on-chip quantum technologies. In particular, we have shown their robustness against an external magnetic field up to 7 T and up to liquid nitrogen temperature, which makes them ideal candidates for circuit-QED experiments with spin ensembles. To display their potentialities, we showed that the collective strong coupling regime of a DPPH ensemble coupled to coplanar YBCO resonators can be achieved up to 40 K.

The authors warmly acknowledge S. Carretta, A. Chiesa, A. Lascialfari, F. Troiani, and M. Barra for useful discussions, T. Orlando for supplementary EPR measurements and S. Marrazzo for fabrication expertise. This work was funded by the Italian Ministry of Education and Research (MIUR) through “Fondo Investimenti per la Ricerca di Base” (FIRB) Project RBF12RPD1, and by the U.S. AFOSR/AOARD program, Contract No. FA2386-13-1-4029.

- <sup>1</sup>Z.-L. Xiang, S. Ashhab, J. Q. You, and F. Nori, *Rev. Mod. Phys.* **85**, 623 (2013).  
<sup>2</sup>C. Grezes, B. Julsgaard, Y. Kubo, M. Stern, T. Umeda, J. Isoya, H. Sumiya, H. Abe, S. Onoda, T. Ohshima *et al.*, *Phys. Rev. X* **4**, 021049 (2014).  
<sup>3</sup>A. Megrant, C. Neill, R. Barends, B. Chiaro, Y. Chen, L. Feigl, J. Kelly, E. Lucero, M. Mariantoni, P. J. J. O’Malley *et al.*, *Appl. Phys. Lett.* **100**, 113510 (2012).  
<sup>4</sup>Z. K. Mineev, I. M. Pop, and M. H. Devoret, *Appl. Phys. Lett.* **103**, 142604 (2013).  
<sup>5</sup>D. F. Walls and G. J. Milburn, *Quantum Optics* (Springer, New York, 2008).  
<sup>6</sup>R. J. Thompson, G. Rempe, and H. J. Kimble, *Phys. Rev. Lett.* **68**, 1132 (1992).  
<sup>7</sup>M. Brune, F. Schmidt-Kaler, A. Maali, J. Dreyer, E. Hagley, J. M. Raimond, and S. Haroche, *Phys. Rev. Lett.* **76**, 1800 (1996).  
<sup>8</sup>A. Wallraff, D. I. Schuster, A. Blais, L. Frunzio, R.-S. Huang, J. Majer, S. Kumar, S. M. Girvin, and R. J. Schoelkopf, *Nature* **431**, 162 (2004).  
<sup>9</sup>K. Hennessy, A. Badolato, M. Winger, D. Gerace, M. Atatüre, S. Gulde, S. Fält, E. Hu, and A. Imamoglu, *Nature* **445**, 896 (2007).  
<sup>10</sup>R. H. Dicke, *Phys. Rev.* **93**, 99 (1954).  
<sup>11</sup>A. Imamoglu, *Phys. Rev. Lett.* **102**, 083602 (2009).  
<sup>12</sup>M. Tavis and F. W. Cummings, *Phys. Rev.* **170**, 379 (1968).  
<sup>13</sup>Y. Kubo, F. R. Ong, P. Bertet, D. Vion, V. Jacques, D. Zheng, A. Dréau, J. F. Roch, A. Auffèves, F. Jelezko *et al.*, *Phys. Rev. Lett.* **105**, 140502 (2010).  
<sup>14</sup>R. Amsüss, C. Koller, T. Nöbauer, S. Putz, S. Rotter, K. Sandner, S. Schneider, M. Schramböck, G. Steinhauser, H. Ritsch *et al.*, *Phys. Rev. Lett.* **107**, 060502 (2011).  
<sup>15</sup>D. I. Schuster, A. P. Sears, E. Ginossar, L. DiCarlo, L. Frunzio, J. J. L. Morton, H. Wu, G. A. D. Briggs, B. B. Buckley, D. D. Awschalom, and R. J. Schoelkopf, *Phys. Rev. Lett.* **105**, 140501 (2010).

- <sup>16</sup>G. R. Eaton and S. S. Eaton, in *Multifrequency Electron Paramagnetic Resonance*, edited by S. K. Misra (Wiley-VCH, Weinheim, 2011).  
<sup>17</sup>D. Zilic, D. Pajic, M. Juric, K. Molcanov, B. Rakvin, P. Planinic, and K. Zadro, *J. Magn. Reson.* **207**, 34 (2010).  
<sup>18</sup>A. M. Prokhorov and V. B. Fedorov, *Sov. Phys. JEPT* **16**, 1489 (1963).  
<sup>19</sup>I. Chiorescu, N. Groll, S. Bertaina, T. Mori, and S. Miyashita, *Phys. Rev. B* **82**, 024413 (2010).  
<sup>20</sup>E. Abe, H. Wu, A. Ardavan, and J. J. L. Morton, *Appl. Phys. Lett.* **98**, 251108 (2011).  
<sup>21</sup>S. Probst, H. Rotzinger, S. Wünsch, P. Jung, M. Jerger, M. Siegel, A. V. Ustinov, and P. A. Bushev, *Phys. Rev. Lett.* **110**, 157001 (2013).  
<sup>22</sup>A. W. Eddins, C. C. Beedle, D. N. Hendrickson, and J. R. Friedman, *Phys. Rev. Lett.* **112**, 120501 (2014).  
<sup>23</sup>G. Boero, G. Gualco, R. Lisowski, J. Anders, D. Suter, and J. Brugger, *J. Magn. Reson.* **231**, 133 (2013).  
<sup>24</sup>M. J. Lancaster, *Passive Microwave Device Applications of High Temperature Superconductors* (Cambridge University Press, Cambridge, 1997).  
<sup>25</sup>M. Hein, *High-Temperature-Superconductor Thin Films at Microwave Frequencies* (Springer, Berlin, 1999).  
<sup>26</sup>G. Ghigo, D. Botta, A. Chiodoni, R. Gerbaldo, L. Gozzelino, F. Laviano, B. Minetti, E. Mezzetti, and D. Andreone, *Supercond. Sci. Technol.* **17**, 977 (2004).  
<sup>27</sup>Th. Kaiser, B. A. Aminov, A. Baumfalk, A. Cassinese, H. J. Chaloupka, M. A. Hein, S. Kolesov, H. Medelius, G. Muller, M. Perpeet *et al.*, *J. Supercond.* **12**, 343 (1999).  
<sup>28</sup>M. Arzeo, F. Lombardi, and T. Bauch, *IEEE Trans. Appl. Supercond.* **25**, 1700104 (2015).  
<sup>29</sup>Y. Tabuchi, S. Ishino, T. Ishikawa, R. Yamazaki, K. Usami, and Y. Nakamura, *Phys. Rev. Lett.* **113**, 083603 (2014).  
<sup>30</sup>X. Zhang, C.-L. Zou, L. Jiang, and H. X. Tang, *Phys. Rev. Lett.* **113**, 156401 (2014).  
<sup>31</sup>E. I. Baibekov, *Opt. Spectrosc.* **116**, 889 (2014).  
<sup>32</sup>A. Ghirri, F. Troiani, and M. Affronte, *Quantum Computation with Molecular Nanomagnets: Achievements, Challenges, and New Trends, Structure and Bonding* (Springer, Berlin, 2014).  
<sup>33</sup>S. Nakazawa, S. Nishida, T. Ise, T. Yoshino, N. Mori, R. D. Rahimi, K. Sato, Y. Morita, K. Toyota, D. Shiomi *et al.*, *Angew. Chem., Int. Ed.* **51**, 9860 (2012).  
<sup>34</sup>A. Collauto, M. Mannini, L. Sorace, A. Barbon, M. Brustolon, and D. Gatteschi, *J. Mater. Chem.* **22**, 22272 (2012).  
<sup>35</sup>M. Warner, S. Din, I. S. Tupitsyn, G. W. Morley, A. M. Stoneham, J. A. Gardener, Z. Wu, A. J. Fisher, S. Heutz, C. W. M. Kay, and G. Aeppli, *Nature* **503**, 504 (2013).  
<sup>36</sup>K. Bader, D. Dengler, S. Lenz, B. Endeward, S. Jiang, P. Neugebauer, and J. van Slageren, *Nat. Commun.* **5**, 5304 (2014).  
<sup>37</sup>See supplementary material at <http://dx.doi.org/10.1063/1.4920930> for detailed description of the experimental procedures, full set of data, and estimation of  $g_s$ .  
<sup>38</sup>D. Bothner, T. Gaber, M. Kemmler, D. Koelle, R. Kleiner, S. Wunsch, and M. Siegel, *Phys. Rev. B* **86**, 014517 (2012).  
<sup>39</sup>J. Krupka, J. Judek, C. Jastrzebski, T. Ciuk, J. Wosik, and M. Zdrojek, *Appl. Phys. Lett.* **104**, 102603 (2014).  
<sup>40</sup>K. Sato, S. Sato, K. Ichikawa, M. Watanabe, T. Honma, Y. Tanaka, S. Oikawa, A. Saito, and S. Ohshima, *J. Phys.: Conf. Ser.* **507**, 012045 (2014).  
<sup>41</sup>J. M. Sage, V. Bolkhovskoy, W. D. Oliver, B. Turek, and P. B. Welander, *J. Appl. Phys.* **109**, 063915 (2011).